Synthesis and Nuclear Magnetic Resonance Study of the Auranonaborane and Diauradecaborane *arachno*-type Compounds, [4-(S_2CNEt_2)-*arachno*-4-AuB_8H_{12}] and [6,9-(S_2CNEt_2)$_2$-*arachno*-6,9-$Au_2B_8H_{10}$]; Crystal and Molecular Structure of [6,9-(S_2CNEt_2)$_2$-*arachno*-6,9-$Au_2B_8H_{10}$] *

Michael A. Beckett, Janet E. Crook, Norman N. Greenwood, and John D. Kennedy
Department of Inorganic and Structural Chemistry, University of Leeds, Leeds LS2 9JT

The reaction of [$AuBr_2(S_2CNEt_2)$] with the *arachno*-[B_9H_{14}]$^-$ anion gives the very pale yellow *arachno* nine-vertex compound [4-(S_2CNEt_2)-4-AuB_8H_{12}] (1) and the bright yellow *arachno* 10-vertex compound [6,9-(S_2CNEt_2)$_2$-6,9-$Au_2B_8H_{10}$] (2) in low yield. Both compounds are characterized by multi element single- and double-resonance n.m.r. spectroscopy, and compound (2), also by single-crystal *X*-ray diffraction analysis. The metal-to-borane bonding mode is similar to that in the iridium and platinum species [1-Cl-4,4,4,4-(PMe_3)$_2$(CO)H-4-IrB_8H_{11}] and [4,4-(PMe_2Ph)$_2$-4-PtB_8H_{12}], to which it is compared.

Many transition metals and post-transition metals have been shown to form air-stable metallaborane species in which the metal atom has been incorporated as a vertex into the cluster.[1-4] Of the heavy transition metals, platinum and iridium have been the most extensively studied; iridium in particular has produced a wealth of novel cluster types as well as valuable insights into cluster bonding.[5] Metallaboranes have also been isolated [5-8] for rhenium, osmium, mercury, and thallium. It is therefore surprising that apart from a report [9] of a rather unstable and ill characterized gold complex, [$Au(B_5H_8)(PPh_3)_n$], there have been no other contiguous auraborane clusters cited in the literature, although it should be pointed out that in metallacarborane chemistry the sequence platinum, gold, mercury, and thallium has been obtained for the formal [$C_2B_9H_{11}$]$^{2-}$ ligand [10-13] and the structure of the [3-(S_2CNEt_2)-3,1,2-$AuC_2B_9H_{11}$] cluster has been determined by *X*-ray diffraction.

We now report that *arachno*-4-auranonaborane and *arachno*-6,9-diauradecaborane clusters can be synthesized from readily available starting materials and that they are air-stable at ambient temperatures. The molecular structure of the *arachno*-6,9-diauradecaborane cluster, as determined by *X*-ray diffraction, is also reported. It is the first structurally characterized auraborane cluster, although again it should be noted that the metal-to-cage bonding in auracarboranes such as [3-(S_2CNEt_2)-3,1,2-$AuC_2B_9H_{11}$] [11] is sustained by gold–boron bonding only.

Results and Discussion

(1) *Preparation.*—The reaction of the gold(III) complex [$AuBr_2(S_2CNEt_2)$] with an excess of [NEt_4][B_9H_{14}] in dichloromethane solution gives two isolable auraborane cluster species, the very pale yellow nine-vertex [4-(S_2CNEt_2)-*arachno*-4-AuB_8H_{12}] (1) and the bright yellow 10-vertex [6,9-(S_2CNEt_2)$_2$-*arachno*-6,9-$Au_2B_8H_{10}$] (2) in (as yet unoptimised) yields of 1 and 5%, respectively [equation (i)]. These novel air-stable auraborane cluster compounds may be isolated chromatographically and have been characterized by multi element n.m.r. experiments and by *X*-ray diffraction for complex (2). Both are solid crystalline compounds at ambient temperatures.

Table 1. Interatomic distances (pm) for [(S_2CNEt_2)$_2$($Au_2B_8H_{10}$)] (2) with estimated standard deviations in parentheses *

Au(6)–S(1)	240.1(3)	Au(6)–S(2)	239.8(3)
Au(6)–B(5)	225.5(13)	Au(6)–B(7)	221.3(13)
Au(6)···Au(9)	358.1(1)	Au(6)–B(2)	221.9(14)
B(1)–B(2)	173.7(18)	B(2)–B(3)	177.6(18)
B(2)–B(5)	182.5(18)	B(2)–B(7)	181.5(19)
B(1)–B(5)	177.6(21)	B(3)–B(7)	182.3(21)
B(5)–B(10)	178.6(28)	B(7)–B(8)	186.7(28)
B(1)–B(3)	175.6(27)		
C(1)–S(1)	174.8(13)	C(1)–S(2)	172.7(12)
C(1)–N	128.7(14)		

* Note: the molecule lies on a crystallographic mirror plane, therefore Au(9) is Au(6′), B(4) is B(2′), B(8) is B(7′), and B(10) is B(5′).

$$[AuBr_2(S_2CNEt_2)] + 2[NEt_4][B_9H_{14}] \longrightarrow \underset{(1)}{[(S_2CNEt_2)(AuB_8H_{12})]} + \underset{(2)}{[(S_2CNEt_2)_2(Au_2B_8H_{10})]} + \text{unidentified degradation products} \quad \text{(i)}$$

This reaction behaviour mimics to some extent that of the isoelectronic *cis*-[$PtCl_2(PMe_2Ph)_2$] complex with [NEt_4][B_9H_{14}] which yields the compound [4,4-(PMe_2Ph)$_2$-4-Pt-B_8H_{12}] from which the species [6,6,9,9-(PMe_2Ph)$_4$-6,9-Pt_2-B_8H_{10}] may in turn be obtained.[14] These have similarities in the metal-to-borane bonding mode to the compounds reported here. [See section (4) below, and Figure 2.] Extensive degradation of the starting borane cluster also presumably occurs but neither gold aggregate clusters nor smaller auraborane clusters have yet been detected or isolated from this reaction mixture.

(2) *Molecular Structure of* [(S_2CNEt_2)$_2$($Au_2B_8H_{10}$)] (2).—Selected interatomic distances for 6,9-bis(*N*,*N*-diethyldithiocarbamato)-6,9-diauradecaborane are given in Table 1, angles between selected interatomic vectors in Table 2, and atomic co-ordinates in Table 3. An ORTEP drawing of the molecular structure is given in Figure 1 and additional detail in Figure 2(*a*). The gross heavy-atom structure of the metallaborane cluster can be seen to be that of an open-faced 10-vertex cluster as found in the 10-vertex decaborane species with either a *nido* electron count (as in $B_{10}H_{14}$ itself) [15] or an *arachno* electron count (as in [$B_{10}H_{14}$]$^{2-}$).[16] These two structural types differ in both the number of bridging

---

* 6,9-Bis(*N*,*N*-diethyldithiocarbamato)-*arachno*-6,9-diauradecaborane.

Supplementary data available (No. SUP 23907, 13 pp.): structure factors, thermal parameters. See Instructions for Authors, *J. Chem. Soc., Dalton Trans.*, 1984, Issue 1, pp. xvii—xix.

Table 2. Angles (°) between interatomic vectors for $[(S_2CNEt_2)_2(Au_2B_8H_{10})]$ (2) with estimated standard deviations in parentheses *

(*i*) At the Au(6) atom			
S(1)–Au–S(2)	74.4(1)	B(7)–Au–B(5)	87.3(5)
B(2)–Au–S(1)	143.4(4)	B(2)–Au–S(2)	139.5(4)
B(5)–Au–S(1)	100.4(3)	B(7)–Au–S(2)	96.4(4)
B(5)–Au–S(2)	170.2(4)	B(7)–Au–S(1)	167.2(4)
B(5)–Au–B(2)	48.1(5)	B(7)–Au–B(2)	48.3(5)
(*ii*) Au(6)–B–B			
Au–B(2)–B(1)	116.9(9)	Au–B(2)–B(3)	117.6(9)
Au–B(2)–B(5)	67.0(6)	Au–B(2)–B(7)	65.6(6)
Au–B(5)–B(1)	113.5(9)	Au–B(7)–B(3)	115.8(9)
Au–B(5)–B(2)	64.9(6)	Au–B(7)–B(2)	66.0(6)
(*iii*) B–B–B			
range 57.7—62.6; mean 60.2			
range 109.2—115.9; mean 112.1			
(*iv*) Other			
S(1)–C(1)–S(2)	113.2(7)		
N–C(1)–S(1)	122.7(9)	N–C(1)–S(2)	123.9(10)

* See footnote to Table 1.

Table 3. Atomic co-ordinates for $[(S_2CNEt_2)_2(Au_2B_8H_{10})]$ (2) with estimated standard deviations in parentheses [a]

Atom	*x*	*y*	*z*
Au(6)	0.236 70(6)	0.149 15(3)	0.169 22(4)
S(1)	−0.050 6(4)	0.111 0(2)	0.040 6(2)
S(2)	0.348 1(4)	0.110 6(2)	−0.042 8(2)
C(1)	0.105 6(17)	0.095 6(6)	−0.088 9(12)
N	0.042 7(12)	0.080 5(6)	−0.208 7(8)
C(2)	−0.166 9(17)	0.068 0(7)	−0.245 1(12)
H(21)	−0.180 9(17)	0.023 7(7)	−0.318 5(12)
H(22)	−0.241 4(17)	0.051 8(7)	−0.157 4(12)
C(3)	−0.257 3(28)	0.139 0(9)	−0.301 8(18)
H(31)	−0.409 7(28)	0.129 2(9)	−0.327 9(18)
H(32)	−0.183 2(28)	0.155 4(9)	−0.389 6(18)
H(33)	−0.243 7(28)	0.183 5(9)	−0.228 5(18)
C(4)	0.179 1(18)	0.075 9(6)	−0.318 2(12)
H(41)	0.102 6(18)	0.092 0(6)	−0.410 4(12)
H(42)	0.299 0(18)	0.114 2(6)	−0.297 4(12)
C(5)	0.260 8(22)	−0.004 7(9)	−0.333 1(14)
H(51)	0.359 3(22)	−0.005 9(9)	−0.413 6(14)
H(52)	0.141 8(22)	−0.043 4(9)	−0.354 5(14)
H(53)	0.338 2(22)	−0.021 1(9)	−0.241 5(14)
B(1)	0.269 1(29)	0.250 0 [b]	0.454 8(19)
B(2)	0.354 7(19)	0.170 6(7)	0.375 3(13)
B(3)	0.509 2(28)	0.250 0 [b]	0.401 8(19)
B(5)	0.100 7(18)	0.199 7(7)	0.348 5(12)
B(7)	0.517 4(18)	0.197 4(7)	0.246 4(12)

[a] See footnote to Table 1. [b] Special position fixed by space-group considerations.

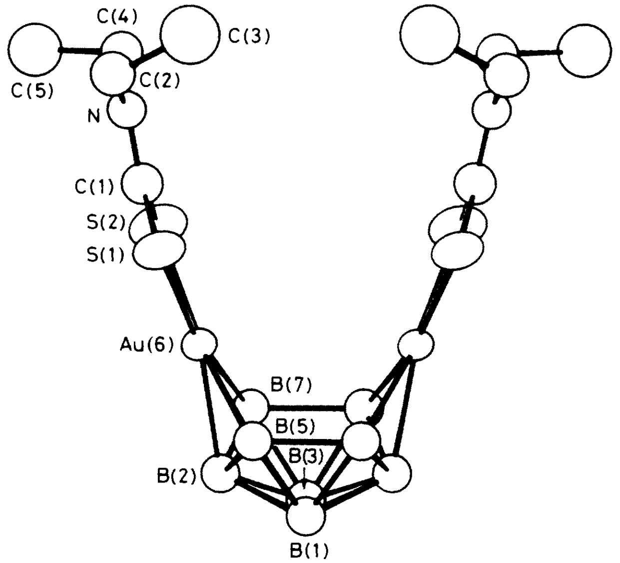

Figure 1. ORTEP drawing of $[(S_2CNEt_2)_2(Au_2B_8H_{10})]$ (2) viewed along the crystallographic mirror plane. Hydrogen atoms were not refined, although peaks in the final difference maps were present at positions for bridging H atoms between B(7) and B(8), and between B(5) and B(10), and for terminal H atoms on all B atoms except B(1) (which lies on the crystallographic mirror plane)

hydrogen atoms and in their relative positions around the open face. For the digold compound (2), n.m.r. spectroscopic evidence [see section (3) below] firmly suggests that each boron atom is bonded to a terminal hydrogen atom and that there are two additional hydrogen atoms which bridge the B(5),B(10) and B(7),B(8) atoms in an identical manner to that found in the *arachno* 10-vertex structures $[B_{10}H_{14}]^{2-}$, $B_{10}H_{12}L_2$,[16] and *arachno*-$[(PMe_2Ph)_4(Pt_2B_8H_{10})]$,[14] consistent with an *arachno* description for this gold species. Peaks corresponding to all the hydrogen atoms except (interestingly) that on B(1) were located on final difference maps, but were not refined.

Inspection of the data in Tables 1—3 shows that the Au_2B_8 cluster and its ligands (apart from their terminal methyl groups) conform closely to an idealized C_{2v} symmetry. The molecule itself lies on a crystallographic mirror plane [through B(1) and B(3) and through the midpoints of the vectors joining B(5) with B(10) and B(7) with B(8)].

The interatomic distances and angles together with the conformation of the *N*,*N*-diethyldithiocarbamate ligand and its interaction with the gold atom are all essentially identical with those reported[11] for the $[(S_2CNEt_2)(AuC_2B_9H_{11})]$ cluster compound and need little further comment. The two $Au(S_2CNEt_2)$ moieties are each bonded to an open triangle of boron atoms and each gold atom is five-co-ordinate. Thus Au(6) is bound to S(1), S(2), B(2), B(5), and B(7). All three boron atoms are, within experimental error, equidistant from the gold atom with an average distance of *ca.* 223 pm. This distance is similar to those reported[11] for the gold–boron distances of 221(2), 223(2), and 220(1) pm for the 12-vertex auracarbaborane mentioned above. The tetragonal bonding plane for the gold atom [defined by Au(6), S(1), and S(2)] intercepts the vector joining B(2) with B(7) and the vector joining B(2) with B(5) in a symmetrical manner. A view looking along this plane from inside the cluster towards the gold and sulphur atoms is shown in Figure 2(*a*) and thus clearly shows the disposition of the symmetric trihapto boron open triangle. Also included in Figure 2 is the analogous view of the platinum vertex in $[4,4\text{-}(PMe_2Ph)_2\text{-}4\text{-}PtB_8H_{12}]$[14] and the iridium vertex in $[1\text{-}Cl\text{-}4,4,4,4\text{-}(PMe_3)_2(CO)H\text{-}4\text{-}IrB_8H_{11}]$[17,18] [see section (4) below].

Several of the boron–boron distances are well within the normal range for polyhedral borane clusters (175—180 pm).[19] The boron–boron distances for B(7)–B(8) and B(5)–B(10) on the open face (average 182 pm) are much shorter than those found in *nido* 10-vertex structures [*e.g.* $B_{10}H_{14}$, 197.3(4) pm][15] and are more typical of distances found in *arachno* 10-vertex decaborane-type structures {*e.g.* $[6,6\text{-}(PPh_3)_2\text{-}6,9\text{-}PtSB_8H_{10}]$, 184.4(28) pm}[20] which is again consistent with the *arachno* description for this cluster. The Au_2B_8 cluster compound can therefore be considered as an analogue of *arachno*-$[B_{10}H_{14}]^{2-}$

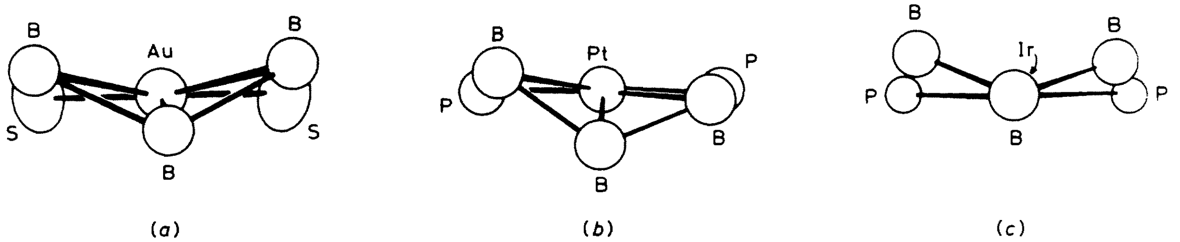

Figure 2. ORTEP drawings of (*a*) the S(1)S(2)Au(6)B(2)B(5)B(7) unit of (2) viewed in the S(1)S(2)Au(6) plane, (*b*) the P(1)P(2)Pt(4)B(1)-B(5)B(9) unit of *arachno*-$[(PMe_2Ph)_2(PtB_8H_{12})]$ viewed in the P(1)P(2)Pt(4) plane, and (*c*) the P(1)P(2)Ir(4)B(1)B(5)B(9) unit of *arachno*-$[(PMe_3)_2(CO)H(IrB_8H_{11}Cl)]$ viewed in the P(1)P(2)Ir(4) plane

Table 4. Selected n.m.r. parameters for $[(S_2CNEt_2)_2(Au_2B_8H_{10})]$ (2) [a]

Assignment [b]	$\delta(^{11}B)$ [c]	Relative intensity	$\delta(^{1}H)$ [d]	Relative intensity	$^{1}J(^{11}B-^{1}H)$/Hz
1,3	−16.9	2	+1.44	2	140 ± 10
2,4	+34.5	2	+5.72	2	120 ± 20
5,7,8,10	+8.7	4	+3.08	4	100 ± 20
Bridge (7,8)(5,10)	—	—	−0.51	2	—
$S_2CN(CH_2CH_3)_2$	—	—	+3.69 [e]	8	—
$S_2CN(CH_2CH_3)_2$	—	—	+1.33 [f]	12	—

[a] In $CDCl_3$ at 21 °C. [b] *arachno*-$B_{10}H_{12}L_2$ numbering system used; see Figure 1. [c] In p.p.m. relative to $BF_3 \cdot OEt_2$ (15% in $CDCl_3$). [d] In p.p.m. relative to $SiMe_4$, terminal ^1H resonances assigned to corresponding boron positions by selective $^1H-\{^{11}B\}$ experiments (refs. 8 and 14). [e] Quartet, $^3J(^1H-^1H)$ *ca.* 7 Hz. [f] Triplet, $^3J(^1H-^1H)$ *ca.* 7 Hz.

Table 5. Selected n.m.r. parameters for $[(S_2CNEt_2)(AuB_8H_{12})]$ (1) [a]

Assignment [b]	$\delta(^{11}B)$ [c]	Relative intensity	$\delta(^{1}H)$ [d]	Relative intensity	$^{1}J(^{11}B-^{1}H)$/Hz
1	+18.9	1	+4.32	1	130 ± 10
2,3	−35.7	2	+0.61	2	150 ± 10
5,9	−15.9	2	+2.25	2	130 ± 20
6,8	−15.9	2	+1.96	2	130 ± 20
7	+9.5	1	+3.56	1	130 ± 10
Bridge (5,6)(8,9)	—	—	−3.03	2	—
Pseudo-bridge (6,8)	—	—	+0.61	2	—
$S_2CN(CH_2CH_3)_2$	—	—	+3.43 [e]	4	—
$S_2CN(CH_2CH_3)_2$	—	—	+1.22 [f]	6	—

[a] In $CDCl_3$ at 21 °C. [b] *arachno*-$B_9H_{13}L$ numbering system used (*iso*-B_9H_{15} cluster type); see Figure 3. [c] In p.p.m. relative to $BF_3 \cdot OEt_2$ (15% in $CDCl_3$). [d] In p.p.m. relative to $SiMe_4$. Terminal proton resonance assigned to boron position by selective $^1H-\{^{11}B\}$ experiments (refs. 8 and 14). [e] Quartet, $^3J(^1H-^1H)$ *ca.* 7 Hz. [f] Triplet, $^3J(^1H-^1H)$ *ca.* 7 Hz.

in which the BH_2^- groups in the 6 and the 9 positions are notionally replaced by the neutral $Au(S_2CNEt_2)$ moieties.

(3) *Nuclear Magnetic Resonance Studies.*—The ^{11}B and ^1H n.m.r. parameters for the diauraborane $[(S_2CNEt_2)_2(Au_2B_8H_{10})]$ (2) are summarized in Table 4. The assignment of the ^{11}B resonances is based upon the general similarity of the spectrum to that of the *arachno*-6,9-diplatinadecaborane $[(PMe_2Ph)_4(Pt_2B_8H_{10})]$,[14] and these assignments indicate high shielding for the 1,3 nuclei and low shielding for the 2,4 nuclei. This is generally observed in *arachno*-decaboranyl species [21–23] which contrasts with the high shielding of the 2,4 nuclei and the lower shielding of the 1,3 nuclei found in *nido* 10-vertex structures.[23,24] This is consistent with the *arachno* description of the cluster as established by the *X*-ray diffraction study discussed above.

The ^{11}B resonance positions in the monoauraborane $[(S_2CNEt_2)(AuB_8H_{12})]$ (1) are also readily assigned by the relative intensities of 2 : 2 : 2 : 1 : 1 and by comparison with those of the *arachno*-4-metallanonaboranes $[(PMe_2Ph)_2(PtB_8H_{12})]$ [14] and $[(PMe_3)_2(CO)H(IrB_8H_{12})]$ [18] and are given together with other selected parameters for this compound in Table 5. The 5,9 and 6,8 positions have accidentally coincident ^{11}B resonances but can be differentiated by noting that two *exo*-terminal proton resonances sharpen when selectively irradiated at $\nu[^{11}B(5,9)(6,8)]$ in $^1H-\{^{11}B\}$ experiments.

For both compounds, the ^1H n.m.r. signals of the borane cluster hydrogen atoms are readily observable in $^1H-\{^{11}B$-(broad band noise)$\}$ experiments, and selective decoupling experiments [8,25,26] then assign their positions and confirm that each boron has a terminal hydrogen atom associated with it (Tables 4 and 5). It is also confirmed that there are two equivalent bridging hydrogen atoms associated with the 5,10;7,8 boron atoms in compound (2) (δ −0.51) and with the 5,6;8,9 boron atoms in compound (1) (δ −3.03), again consistent with the solid-state structure of the Au_2B_8 cluster compound (2) and with the *arachno* description of the bonding for both species. For compound (1) the $^1H-\{^{11}B\}$ selective decoupling experiments also indicate that the *endo*-terminal/pseudo-bridging hydrogen atoms (δ + 0.61) are associated principally with the 6 and 8 positions. Selective irradiation at $\nu[^{11}B(7)]$, for example, produces no selective sharpening of this proton resonance. This selectivity is similar to that found for the two 6,8-*endo*-terminal protons for the *arachno*-nonaborane compound $4-(SMe_2)B_9H_{12}$ [27] which are similarly associated with the 6,8 resonances only. This evidence indicates that compound (1) is reasonably formulated as *arachno*-$[(S_2CNEt_2)(AuB_8H_{12})]$ in a similar manner to the structurally characterized metallanonaboranes *arachno*-$[(PMe_2Ph)_2(PtB_8H_{12})]$ [14] and *arachno*-$[(PMe_3)_2(CO)H(IrB_8H_{11}Cl)]$.[17,18] The proposed structure is shown in Figure 3.

(4) *Bonding Considerations.*—The analogy with the *arachno* nine- and 10-vertex borane species such as $B_9H_{13}L$ and $B_{10}H_{12}L_2$ suggests that the bonding at the metal centre in the auraboranes [structure (II)] mimics the bonding at the equivalent boron centres in the non-metalla species [structure (I)] and that the metal centre consequently contributes two orbitals and two electrons to the cluster bonding. Consistent with this, the square-planar gold(III) bonding environment, as defined by the AuS_2 plane, indicates that the metal-to-borane orbital bonding vectors are directed towards partial three-centre AuBB bonds which will have their maximum electron densities slightly outside the triangular AuB_2 faces [Figure 2(*a*)]. In this it is similar to the bonding in the iridium analogue $[(PMe_3)_2(CO)H(IrB_8H_{11}Cl)]$ [Figure 2(*c*)] (which however probably also exhibits effects due to distortion

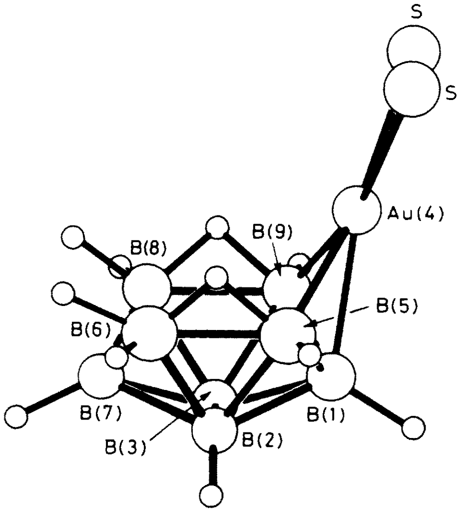

Figure 3. Proposed structure of [$(S_2CNEt_2)(AuB_8H_{12})$] (1) (with $CNEt_2$ grouping omitted). In this projection the *exo*-terminal H atom on B(3) is obscured

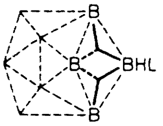

(I)

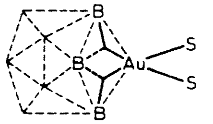

(II)

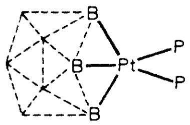

(III)

arising from intramolecular van der Waals effects),[18] but differs somewhat from the platinum analogues [Figure 2(*b*)] which are claimed to have additional metal-to-borane bonding contributions from structures such as (III).[14]

It may be noted that the new gold species reported here could be regarded as inconsistent with cluster electron-counting rules. This is because these rules implicitly count orbitals as well as electrons, so that in structure (I) the electrons in the *endo*-terminal B–H bond are counted even though they do not contribute to the skeletal cluster bonding. In the square-planar gold(III) environment no such valence energy electrons are available in such an *endo*-terminal environment for counting purposes, and so the cluster would have an electron count two short per gold vertex for a formal binary borane *arachno* cluster. Although one could notionally count the essentially non-bonding gold d_{z^2} electron pair for this purpose, this would be rather contrived as in these compounds there is probably little significant contribution to the bonding from the gold(V) valence state. These and analogous considerations are general for ' non-conical ' transition-metal cluster fragments.

Experimental

General.—The gold complex [$AuBr_2(S_2CNEt_2)$] was prepared from $HAuCl_4{\cdot}xH_2O$ by standard methods.[28,29] $B_{10}H_{14}$ was sublimed (0.1 mmHg at 80 °C) before use and [NEt_4][B_9H_{14}] was prepared from it by published methods.[14] Dichloromethane was refluxed over and distilled from CaH_2 prior to use. Nitrogen was dried by passage through concentrated H_2SO_4 and then through KOH pellets.

Preparation of [4-(S_2CNEt_2)-*arachno*-4-AuB_8H_{12}] (1) *and* [6,9-$(S_2CNEt_2)_2$-*arachno*-6,9-$Au_2B_8H_{10}$] (2).—A solution of [NEt_4][B_9H_{14}] (0.430 g, 2.0 mmol) in dry CH_2Cl_2 (20 cm^3) was prepared at room temperature under an atmosphere of dry N_2. To this was added [$AuBr_2(S_2CNEt_2)$] (0.590 g, 1.0 mmol) by use of a tipper tube. The initially orange solution rapidly darkened and was stirred for 30 min. Subsequent manipulations were carried out in air. The reaction mixture was filtered through silica (2 g) which was then washed thoroughly with *ca.* 30 cm^3 of dry CH_2Cl_2. The filtrate was reduced to *ca.* 2 cm^3 in volume under reduced pressure (water pump) at room temperature and applied to a series of preparative t.l.c. plates (Kieselgel GF 254; Fluka AG) which were eluted with a CH_2Cl_2–light petroleum (b.p. 60—80 °C) (80 : 20) mixed-solvent system. The bright yellow component (R_f 0.9) was removed from the t.l.c. plates, washed from the silica by *ca.* 30 cm^3 of dry CH_2Cl_2, and reduced in volume to *ca.* 2 cm^3 as before. Further application of this component to preparative t.l.c. plates followed by elution with C_6H_6 (100%) separated this fraction into two main components: (*i*) a colourless band (seen under u.v. illumination), R_f 0.7; and (*ii*) a yellow band, R_f 0.5. These were taken from the plate and removed from the silica by washing with *ca.* 30 cm^3 of dry CH_2Cl_2 each to give the two compounds, pure by n.m.r. spectroscopic analysis, [$(S_2CNEt_2)(AuB_8H_{12})$] (R_f 0.7) [compound (1)] and [$(S_2CNEt_2)_2(Au_2B_8H_{10})$] ($R_f$ 0.5) [compound (2)] in yields, based on the gold starting complex, of 1 and 5% respectively. A crystal of the latter compound, suitable for *X*-ray diffraction analysis, was grown by diffusion of solvents (CH_2Cl_2–cyclohexane) at room temperature.

Crystal Data for [$(S_2CNEt_2)_2(Au_2B_8H_{10})$] (2).—$C_8H_{30}Au_2B_8N_2S_4$, $M = 763.0$, monoclinic, $a = 0.686\,2(2)$, $b = 1.775\,1(7)$, $c = 1.005\,0(3)$ nm, $\beta = 92.82(3)°$, $U = 1.222\,8(7)$ nm^3, $Z = 2$, $D_c = 2.072$ Mg m^{-3}, $F(000) = 708$, space group $P2_1/m$, Mo-K_α radiation (graphite monochromatized), $\lambda = 71.069$ pm, μ(Mo-K_α) = 12.114 m^{-1}.

Structure Determination of (2).—Measurements were made on a Syntex $P2_1$ diffractometer. Cell dimensions and their standard deviations were obtained by least-squares treatment of the setting angles of 15 reflections having $35 < 2\theta < 40°$. The intensities of all independent reflections in the range $4 < 2\theta < 45°$ were measured in the ω–2θ scan mode with scan speeds varying between 1 and 29° min^{-1} according to a pre-scan intensity and running from 1° below $K_{\alpha 1}$ to 1° above $K_{\alpha 2}$. After correction for Lorentz, polarisation, and transmission factors [$T = 0.0394$—0.1620] 1 565 reflections with $I > 2\sigma(I)$ were retained for the structure analysis; 72 below this threshold were rejected as ' unobserved '. The structure was solved from Patterson and difference syntheses which confirmed that the space group was $P2_1/m$. Full-matrix least-squares refinement, with anisotropic thermal parameters for the gold and sulphur atoms, converged at $R = 0.043$. The ethyl hydrogen atoms were included in the refinement as part of the rigid groups allowed by the SHELX program giving $R = 0.041$. All the borane hydrogens, except that bonded to B(1) were located on a difference map. However, they could not be properly refined and the structure analysis was terminated at the stage mentioned above. Atomic scattering factors were calculated using the analytical approximation and coefficients given in ref. 30. Least-squares weights were obtained from $w^{-1} = \sigma^2(F)$ as carried out by the SHELX program.

Nuclear Magnetic Resonance Spectroscopy.—100-MHz ^{1}H and ^{1}H-{^{11}B}, and 32-MHz ^{11}B and ^{11}B-{^{1}H} experiments were carried out on a JEOL FX-100 pulse Fourier-transform (F.t.) spectrometer.[8,26] High field (128 MHz) ^{11}B and ^{11}B-{^{1}H} experiments were performed on a Bruker WH-400 pulse F.t. spectrometer as part of the S.E.R.C. service at Sheffield. Solution and conditions are specified in Tables 4 and 5. Chemical shifts (δ) are given in p.p.m. to high frequency (low field) of $SiMe_4$ for ^1H and in p.p.m. to high frequency (low field) of $BF_3{\cdot}OEt_2$ (Ξ 32 083 971 Hz) for ^{11}B.

Acknowledgements

We thank the S.E.R.C. for support, Drs. J. Bould and J. D. Woollins for discussions, and Johnson Matthey Chemicals for the loan of gold compounds.

References

1 N. N. Greenwood and J. D. Kennedy, in 'Metal Interactions with Boron Clusters,' ed. R. N. Grimes, Plenum Press, New York, 1982, ch. 2, pp. 43—118.

2 R. N. Grimes, in 'Comprehensive Organometallic Chemistry,' eds. G. Wilkinson, F. G. A. Stone, and E. W. Abel, Pergamon, Oxford, 1982, vol. 1, ch. 5.5, pp. 459—543.

3 K. B. Gilbert, S. K. Boocock, and S. G. Shore, in 'Comprehensive Organometallic Chemistry,' eds. G. Wilkinson, F. G. A. Stone, and E. W. Abel, Pergamon, Oxford, 1982, vol. 6, ch. 14.1, pp. 879—945.

4 J. D. Kennedy, *Prog. Inorg. Chem.*, 1984, **32**, 519.

5 J. Bould, N. N. Greenwood, and J. D. Kennedy, *J. Organomet. Chem.*, 1983, **249**, 11 and refs. therein.

6 J. W. Lott and D. F. Gaines, *Inorg. Chem.*, 1974, **13**, 2261.

7 N. N. Greenwood, B. S. Thomas, and D. W. Waite, *J. Chem. Soc., Dalton Trans.*, 1975, 299.

8 M. A. Beckett and J. D. Kennedy, unpublished work.

9 N. N. Greenwood and J. Staves, *J. Chem. Soc., Dalton Trans.*, 1978, 1144.

10 D. M. P. Mingos, M. I. Forsyth, and A. J. Welch, *J. Chem. Soc., Dalton Trans.*, 1978, 1363.

11 H. M. Colquhoun, T. J. Greenhough, and M. G. H. Wallbridge, *J. Chem. Soc., Dalton Trans.*, 1978, 303.

12 H. M. Colquhoun, T. J. Greenhough, and M. G. H. Wallbridge, *J. Chem. Soc., Dalton Trans.*, 1979, 619.

13 H. M. Colquhoun, T. J. Greenhough, and M. G. H. Wallbridge, *J. Chem. Soc., Chem. Commun.*, 1976, 1019.

14 S. K. Boocock, N. N. Greenwood, M. J. Hails, J. D. Kennedy, and W. S. McDonald, *J. Chem. Soc., Dalton Trans.*, 1981, 1415.

15 A. Tippe and W. C. Hamilton, *Inorg. Chem.*, 1969, **8**, 464.

16 D. S. Kendall and W. N. Lipscomb, *Inorg. Chem.*, 1973, **12**, 546.

17 J. Bould, J. E. Crook, N. N. Greenwood, J. D. Kennedy, and W. S. McDonald, *J. Chem. Soc., Chem. Commun.*, 1982, 346.

18 J. Bould, J. E. Crook, N. N. Greenwood, and J. D. Kennedy, *J. Chem. Soc., Dalton Trans.*, in the press.

19 N. N. Greenwood and B. S. Thomas, in 'Comprehensive Inorganic Chemistry,' eds. J. C. Bailar, H. J. Emeléus, R. Nyholm, and A. F. Trotman-Dickenson, Pergamon, Oxford, 1973, vol. 1, ch. 11, pp. 665—991.

20 D. A. Thompson, T. K. Hilty, and R. W. Rudolph, *J. Am. Chem. Soc.*, 1977, **99**, 6774.

21 E. L. Muetterties, *Inorg. Chem.*, 1963, **2**, 647.

22 D. E. Hyatt, F. R. Scholer, and L. J. Todd, *Inorg. Chem.*, 1967, **6**, 630.

23 M. A. Beckett and J. D. Kennedy, *J. Chem. Soc., Chem. Commun.*, 1983, 575.

24 A. O. Clouse, D. C. Moody, R. R. Rietz, T. Roseberry, and R. Schaeffer, *J. Am. Chem. Soc.*, 1973, **95**, 2496.

25 J. D. Kennedy and N. N. Greenwood, *Inorg. Chim. Acta*, 1980, **35**, 93.

26 J. D. Kennedy, unpublished work.

27 J. E. Crook, N. N. Greenwood, J. D. Kennedy, and W. S. McDonald, *J. Chem. Soc., Dalton Trans.*, in the press.

28 S. Åkerström, *Arkiv. Kemi*, 1959, **14**, 387.

29 H. A. J. Blaauw, R. J. F. Nivard, and G. J. M. Van der Kerk, *J. Organomet. Chem.*, 1964, **2**, 236.

30 'International Tables for *X*-Ray Crystallography,' Kynoch Press, Birmingham, 1974, vol. 4.

Received 30*th September* 1983; *Paper* 3/1731